Research Article

Investigation of structure and rheological behavior of a new epoxy polymer pentaglycidyl ether pentabisphenol A of phosphorus and of its composite with natural phosphate

Rachid Hsissou[1] · Omar Dagdag[1] · Mohamed Berradi[1] · Mehdi El Bouchti[2] · Mohammed Assouag[3] · Abderrahim El Bachiri[4] · Ahmed Elharfi[1]

Abstract
Novel pentafunctional epoxy resin, mainly based on pentaglycidyl ether pentabisphenol A of phosphorus (PGEPBAP) has been synthesized and characterized through different spectroscopic methods (FTIR, ^{1}H NMR, ^{13}C NMR and ^{31}P NMR). Moreover, the analysis of the viscosity of (PGEPBAP/Methanol) system was determined by using viscosimeter VB-1423 of the Ubbelohde type. Furthermore, the analysis of the rheological properties of the matrix PGEPBAP and their (PGEPBAP/MDA/PN) elaborated composite was performed according the RHM01-RD HAAKE rheometer. In addition, the morphology of different (PGEPBAP/MDA/PN) prepared composite was determined by using the polarizing optical microscope.

Keywords Epoxy resin · PGEPBAP · Viscosity · Rheology · Composite

1 Introduction

The polymers exhibit a rather particular rheological behavior when compared to other materials because of exhibiting viscosimetric behavior in the solid state and in the molten state [1, 2]. The rheological evaluation of the epoxy resin and its composite under the conditions of the processing by injection is useful for the control of the quality of the material and at the same time for further improving the product. Furthermore, epoxy resins and their composites can behave like Newtonian low shear fluids and non-Newtonian high-shear fluids [3, 4]. The rheological analysis investigates the deformation of bodies under the effect of the applied stresses makes it possible to determine the relation between the shear stress and the deformation according to the shear time [5]. The products preparation process of (liquids, gels, pastes, …) or the shaping of the parts (in metallurgy, in plastics, …) invariably require the study of the considered material flow. Therefore, it is necessary to know the behavior of the material to determine the forces involved [6]. Depending on the nature of the fluid to be studied, numerous viscosimeter have been developed, however the technical requirements of the melted resin rheometer such as the high temperature thermal regulation and the obtaining of shear rates close to the industrial conditions of the setting in shape strongly limit the choice of these instruments [7]. Machines developed on extruders and equipped with flat dies allow both the determination of viscosity and rheology studies but at low shear rate [8].

✉ Rachid Hsissou, r.hsissou@gmail.com | [1]Laboratory of Agricultural Resources, Polymers and Process Engineering (LARPPE), Team of Polymer and Organic Chemistry (TPOC), Department of Chemistry, Faculty of Sciences, Ibn Tofail University, BP 133, 14000 Kenitra, Morocco. [2]Laboratory REMTEX, ESITH (Hight School of Textile and Clothing Industries), Casablanca, Morocco. [3]Team of Materials, Metallurgy and Process Engineering, ENSAM, University Moulay Ismail, Al Mansour, B.P. 15290, Meknes, Morocco. [4]Royal Naval School, University Department, Boulevard Sour Jdid, Casablanca, Morocco.

SN Applied Sciences (2019) 1:869 | https://doi.org/10.1007/s42452-019-0911-8

Received: 26 February 2019 / Accepted: 11 July 2019 / Published online: 18 July 2019

2 Materials and methods

All the employed chemicals were purchased from Aldrich Chemical Co.

2.1 Synthesis of pentaglycidyl ether pentabisphenol A of phosphorus PGEPBAP

The synthesis of the epoxy resin named pentaglycidyl ether pentabisphenol A of phosphorus (PGEPBAP) was carried out in two steps according to Hsissou et al. [9].

The first step consists of condensing 0.004 mol of phosphorus pentachloride with 0.026 mol of bisphenol A in the presence of the 4.274 mol of methanol with magnetic stirring for 48 h at 100 °C. The reaction scheme is shown in Fig. 1.

In the second step, 3.014 mol of epichlorohydrin were added to the previously obtained solution of pentahydroxy pentabisphenol A ether phosphoric under magnetic stirring for 4 h at 70 °C. The synthesis of the epoxy resin named pentaglycidyl ether pentabisphenol A of phosphorus is finalized by adding 3.241 mol of triethylamine base with magnetic stirring for 3 h at 40 °C. The reaction scheme is presented in Fig. 2. The methanol solvent as well as the excessive triethylamine base was removed using the rotary evaporator. The triethylammonium chloride by-product was removed by dissolving the crude product in tetrahydrofuran, followed by filtration and solvent evaporation. Typical yield was 85%.

2.2 Hardening the pentafunctional epoxy resin PGEPBP with methylene dianiline

The polyepoxide architecture can be converted into a thermosetting matrix via the methylene dianiline acting as a hardener during the implementation. Methylene dianiline has a very good thermal stability and lends very good mechanical properties to the pre-polymerized resin (epoxide + hardener) [9] this is why they are often used for high-tech applications. Methylene dianiline are bearing two amine functions among which the four hydrogens can be substituted. The formation of the three-dimensional network mainly involves condensations reactions between the oxirane rings of the epoxy resins and the amine functions of the hardener (Fig. 3) [10].

The cure protocol consists of preheating the approximately stoichiometric amounts of the epoxy resin and the hardener. The methylene dianiline is put in an oven at 120 °C, while the epoxy resin PGEPBAP is brought to 60 °C. Thereafter, both molten components are mixed and cured in a mold at 60 °C for 2 h. Moreover, we applied the same protocol for the.

crosslinking reaction of the epoxy resin PGEPBAP in the presence of methylene dianiline as a hardener and natural phosphate at different percentages (0%, 5%, 10% and 15%) as a filler to get a composite (PGEPBAP/MDA/PN). Then, we obtained samples with the well dispersed filler in the base matrix PGEPBAP after a major stir [11]. Natural phosphate composition is $Ca_5(PO_4)_3(OH)$, $Ca_5(PO_4)_3F$ and $Ca_5(PO_4)_3Cl$ with average grain size 0.06 µm.

2.3 Calculation of the stoichiometric coefficients ratio

We hardened the pentafunctional epoxy resin; pentaglycidyl ether pentabisphenol A of phosphorus (PGEPBAP) in the presence of methylene dianiline as a hardener at approximately stoichiometric amounts [9]. The equivalent epoxy weight (EEW) and the amine hydrogen equivalent weight (AHEW) are calculated according to Eqs. 1 and 2. Furthermore, the ratio by weight of the hardener relative

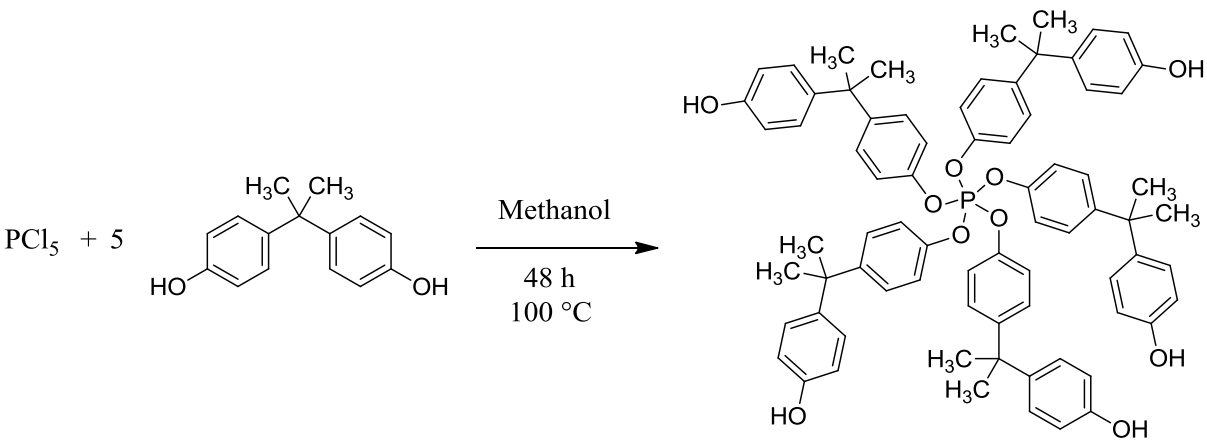

Fig. 1 Synthesis of pentahydroxy pentabisphenol A ether phosphoric

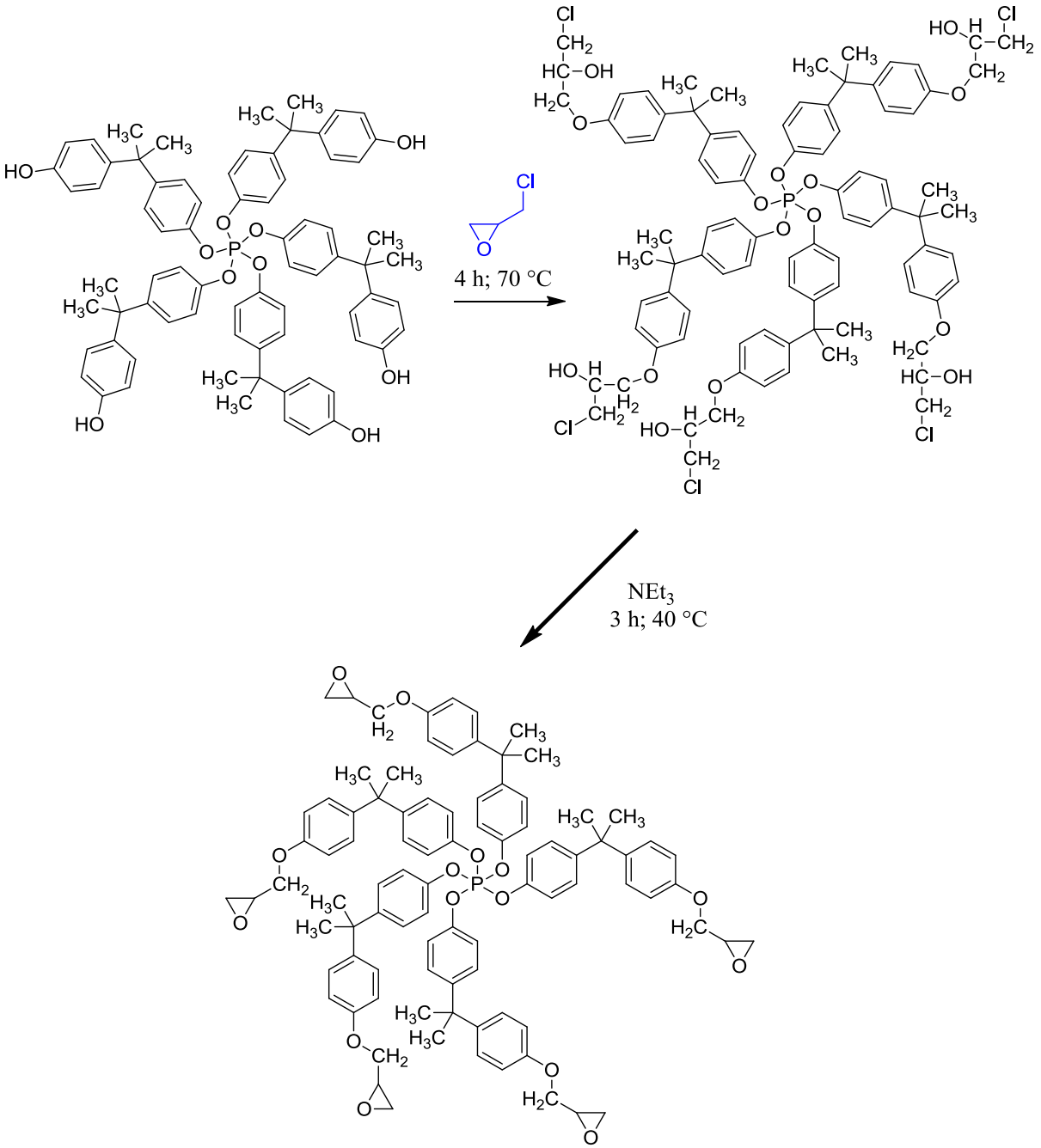

Fig. 2 Synthesis of pentaglycidyl ether pentabisphenol A of phosphorus

to the epoxy resin is calculated in the majority of cases per 100 parts of the resins or parts per hundered of resin (PHR) (Eq. 3). Thus, the amount of the desired charge is calculated using Eq. 4.

$$EEW = \frac{M_w(PGEPBAP)}{f} \quad (1)$$

$$AHEW = \frac{M_w(MDA)}{f} \quad (2)$$

$$PHR = \frac{AHEW}{EEW} \times 100 \quad (3)$$

$$y\% = \frac{x}{resin + MDA + x} \quad (4)$$

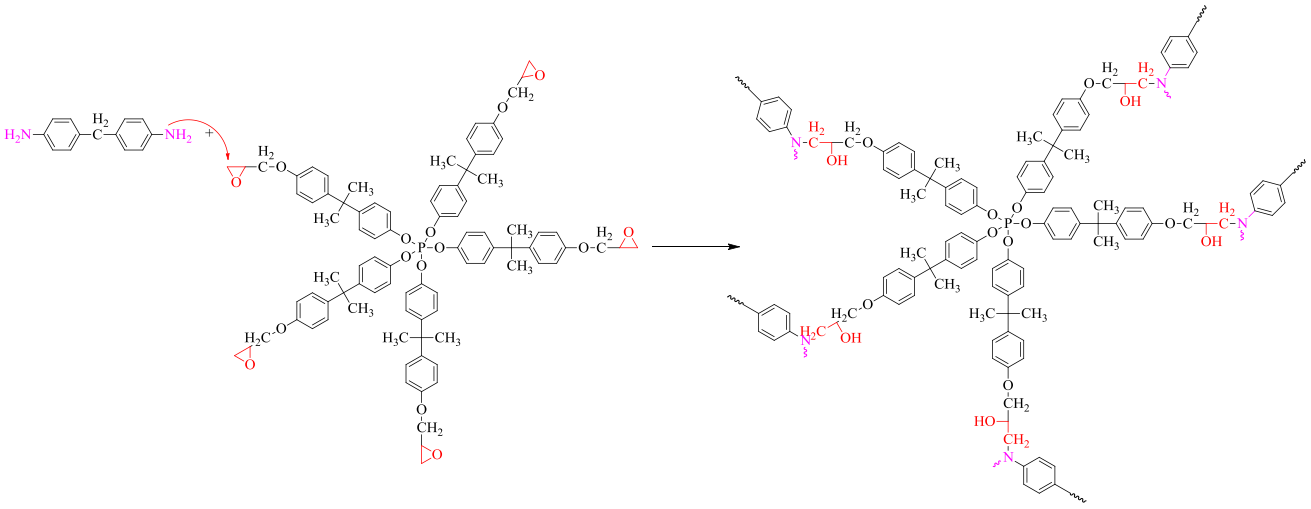

Fig. 3 Structure of pentaglycidyl ether pentabisphenol A of phosphorus crosslinked with methylene dianiline

with f is the functionality of the epoxy resin PGEPBAP, x is the amount of the PGEPBAP and y is the amount of the natural phosphate load.

2.4 Fourier transform infrared spectroscopy

The infrared spectrometer used is BRUKER Fourier transformed infrared spectrometer (FTIR). The light beam passes through the sample to a thickness of 2 µm. The analysis is carried out between 4000 and 600 cm^{-1}.

2.5 Nuclear magnetic resonance

The nuclear magnetic resonance analyzes (^{1}H NMR, ^{13}C NMR and ^{31}P NMR) were obtained by using the BRUKER AVANCE 300 MHz apparatus. The used solvent is deuterated DMSO (DMSO-d6) and the chemical displacements are expressed in ppm.

2.6 Viscosimetric behavior

The analysis of the viscosity of the pentafunctional epoxy resin of (PGEPBAP/Methanol) system was determined using capillary viscosimeter VB-1423 of the Ubbelohde type.

2.7 Rheological behavior

The analysis of the rheological properties of the new macromolecular pentafunctional phosphoric epoxy resin (PGEPBAP) and its composite (PGEPBAP/MDA/PN) was followed by using a RHM01-RD HAAKE rheometer type.

2.8 Polarizing optical microscope

This polarizing optical microscope (POM) is composed of a lens optics system in order to obtain an enlarged image of the sample to be observed. The latter is an optical instrument which is equipped with an object and an eyepiece that makes it possible to magnify the image of a small object and to separate the details of this image so it becomes observable by the human eye.

3 Results and discussion

3.1 Characterization of epoxy resin PGEPBAP

The structural analysis of the synthesized pentafunctional epoxy resin PGEPBAP was determined by Fourier Transform Infrared spectroscopy (FTIR). Its chemical structure was confirmed by nuclear magnetic resonance (^{1}H NMR, ^{13}C NMR and ^{31}P NMR).

3.2 Fourier transform infrared spectroscopy

The synthesized epoxy resin was characterized by Fourier transform infrared analysis. The latter has been exposed in its viscous state to infrared radiation in ATR mode. The different bands of the synthesized pentafunctional epoxy resin PGEPBAP are given in Table 1.

3.3 Nuclear magnetic resonance

The structure of the pentafunctional epoxy resin PGEPBAP synthesized was confirmed by (^{1}H NMR, ^{13}C NMR and ^{31}P NMR). The letters s, d, t, q, and m signify singlet, doublet,

Table 1 Different bands of IR spectrum of epoxy resin PGEPBAP

Band υ (cm^{-1})	Attribution
3224	Bond stretching, Csp^2 (C–H aromatic)
2969	Bond stretching, C–H in CH_3 group
2875–2931	Bond stretching, CH_2 (aliphatic)
1510	Bond stretching, Csp^2 (C=C aromatic)
1246	Bond stretching, C–O aromatic ethers (Ph–O)
1181	Bond stretching, P–O
1041	Bond stretching, C–O aliphatic ethers (CH_2–O)
880	Bending of CH_2 (epoxy)
794–832	Bending of C–H aromatic (Csp^2)

triplet, quadruplet, and multiplet, respectively. The attribution of different chemical shifts of the synthesized epoxy resin PGEPBAP is as follows.

^{1}H RMN (ppm): 1.2 (s, 30 H, CH_3); 3.2 (d, 10 H, CH_2 of oxirane); 3.4 (m, 5H, CH of oxirane); 4.3 (d, 10H, CH_2 related to oxirane); 6.7–6.8 (d, 20H, CH aromatic linked to oxygen) and 7–7.3 (d, 20H, CH aromatic linked to carbon).

^{13}C RMN (ppm): 30 (s, 10 C, CH_3); 42 (s, 5C, quaternary carbon); 48 (s, 5C, CH of oxirane); 54 (s, 5C, CH_2 of oxirane); 65 (s, 5C, CH_2 linked to oxirane); 115 (s, C, ortho aromatic carbon of the glycidyl group); 119 (s, C, ortho aromatic carbon of the O–P group); 128 (s, C, aromatic meta of the glycidyl group); 132 (s, C, aromatic meta of the O–P group); 142 (s, C, aromatic carbon linked to quaternary carbon); 157 (s, C, aromatic carbon linked to oxygen).

^{31}P NMR (ppm): 1.331 (s, P)—this supports the five-armed phosphorus structure.

3.4 Viscosity in dependence of solution concentration and temperature

In order to determine the viscosity of the pentafunctional epoxy resin synthesized: pentaglycidyl ether pentabisphenol A of phosphorus (PGEPBAP) as a function of solution concentration and temperature, we dissolved this epoxy resin in methanol at different concentrations (5%, 10% and 15%). Then, we studied the viscosity of (PGEPBAP/Methanol) system using Ubbelohde VB-1423 capillary viscosimeter at variable temperatures (30–70 °C). Figure 4 shows the viscosity according to the solution concentration (a) and temperature (b), respectively. From Fig. 4a, we observed that the variation of the viscosity increases with the increase of the solution concentration of epoxy resin in the (PGEPBAP/Methanol) system. This is due to the effect of concentration of the branched epoxide molecules. It was also previously observed that the viscosity increases with the increase of the molecular weight of the (PGEPBAP/Methanol) system [12]. In Addition, the viscosity decreases with increasing trend of temperature; this implies that the pentafunctional epoxy resin PGEPBAP changes from a viscous state to a liquid state. This is explained by the heat generated by the apparatus which weakens the interaction between the links (Fig. 4b) [13].

3.5 Shear stress in dependence of the velocity gradient

Figure 5 shows the variation of the shear stress according to the velocity gradient. From this figure, we observed that the shear stress increases with increasing the velocity gradient. The latter is studied using a RHM01-RD

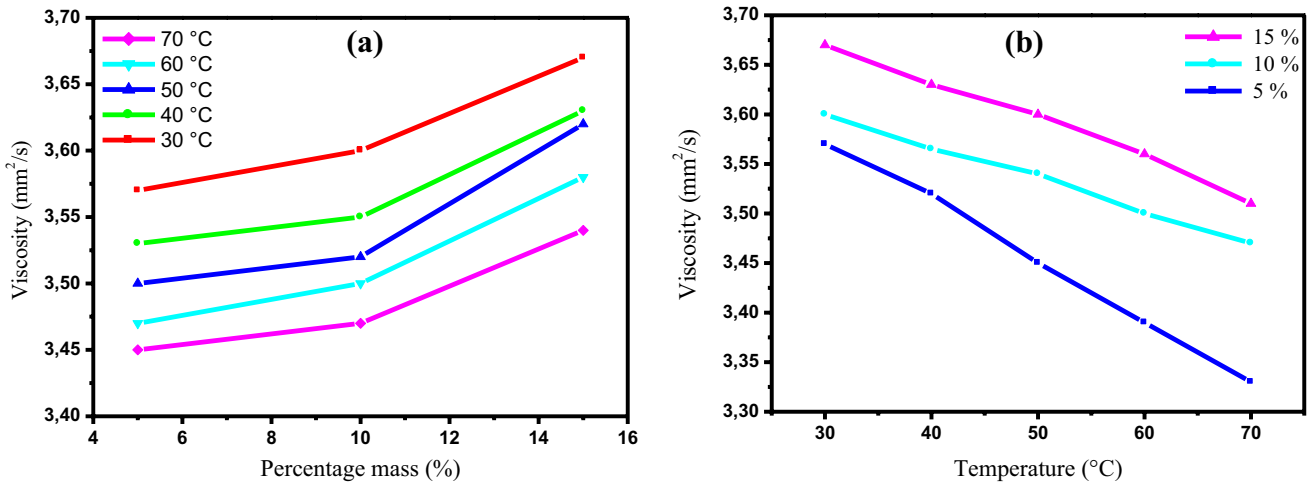

Fig. 4 Viscosity of (PGEPBAP/Methanol) system as a function of solution concentration (**a**) and temperature (**b**)

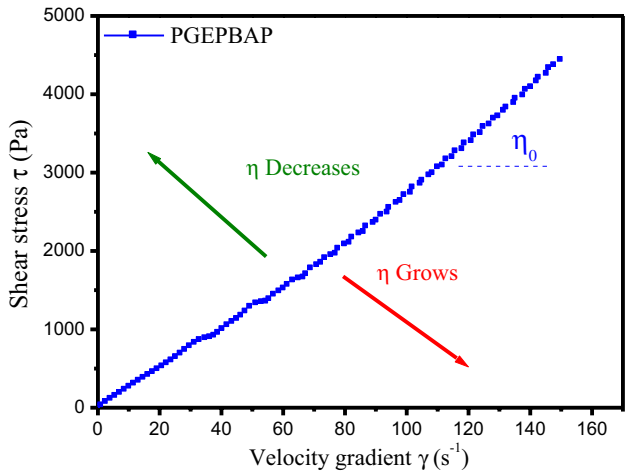

Fig. 5 Shear stress according to the velocity gradient

HAAKE rheometer type. Moreover, for a Newtonian fluid, the viscosity does not depend on the velocity gradient, which means that by representing the shear stress as a function of the velocity gradient. Then, we obtained a line that passes through the origin, whose slope value is the viscosity, as denoted by η_0 [14].

3.6 Viscosity in dependence of temperature

Figure 6 present the viscosity of the pentafunctional phosphoric epoxy resin PGEPBAP according to the temperature. The latter is studied using a RHM01-RD HAAKE rheometer type. Then, the pseudo-plastic model takes into account the variation of the viscosity as a function of temperature [15, 16]. A slight increase in temperature induces a decrease in viscosity due to a significant increase in the molecular mobility of the epoxy resin chains because of the heat provided by the apparatus. As will be discussed below this also accelerates the homopolymerization process of the pentafunctional phosphorus matrix (high concentration: 100% + high temperature: 100–140 °C), which, however is not visible in Fig. 6. The glass transition occurs in the range 70–120 °C, followed by a melt region (low viscosity) [17, 18]. Furthermore, the viscosity strongly depends on the temperature to maintain a sense of the extent to which we specify the temperature at which it was made. In a liquid, the viscosity decreases rapidly depending on the temperature [19, 20].

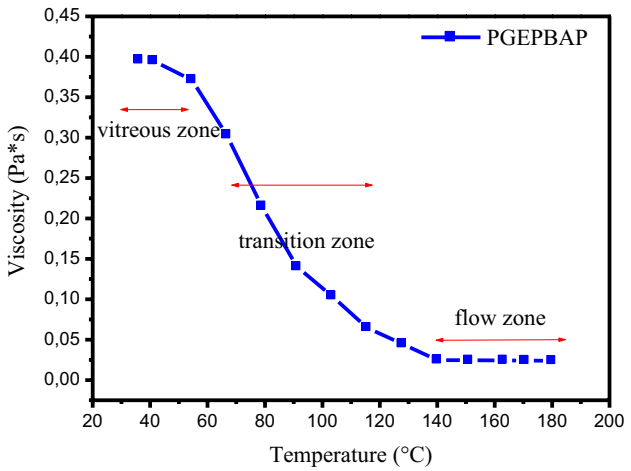

Fig. 6 Viscosity according to the temperature

3.7 Storage modulus and loss modulus

3.7.1 Storage modulus and loss modulus-temperature dependence

Figure 7 shows the storage modulus G′ and loss modulus G″ of the epoxy resin PGEPBAP in dependence of the temperature, respectively. These latter are studied using a RHM01-RD HAAKE rheometer type. From this figure, we found that the values of the storage modulus G′ and loss modulus G″ increase with the increase of the temperature up to the glass transition temperature. Above the latter, the storage modulus and the loss modulus diminish again. At temperatures below the glass transition temperature, the response generally is of the gel type. The cold resin is rigid below Tg. Interestingly, temperature increase does not lead to softening but to stiffening this can be explained by homo-polymerization, which gains importance with increasing temperature (and which is supported by the high concentration—100% of the penta-epoxide). Below Tg, the homo-polymerizing resin is glassy, hence the steep increase of the modulus. Above Tg, the

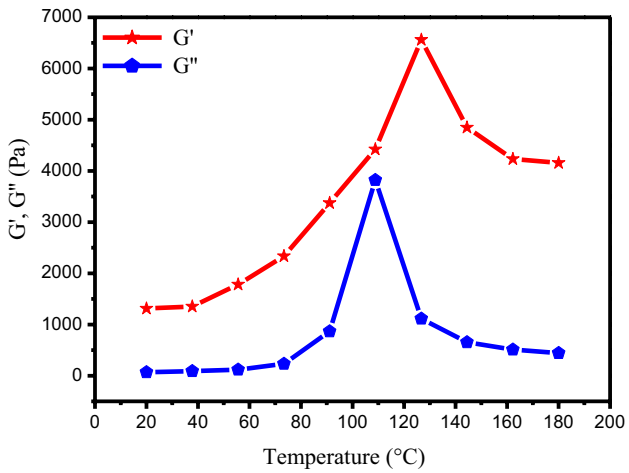

Fig. 7 Storage modulus and loss modulus according to the temperature

homo-polymerizing resin becomes rubbery, the loss modulus dramatically decreases, while the storage modulus assumes a value typical of a very soft rubber (the homo-polymerization still is not quantitative at this point). The values of the glass transition temperature deduced from the trends of the storage modulus and loss modulus are equal to: 127 and 108 °C, respectively.

3.7.2 Thermodynamic parameters

The following method was used to estimate the activation energy associated with the rheological behavior process [21, 22]. This consists of determining the activation energy by using the Eq. 5. Moreover, the activation enthalpy variation ΔH_a and the activation entropy variation ΔS_a are calculated according to the Eqs. 6 and 7. In addition, the activation of the free energy variation ΔG_a is the difference between the ΔH_a and ΔS_a (Eq. 8).

$$G = G_0 \exp\left(-\frac{E_a}{RT}\right) \tag{5}$$

$$G = \frac{RT}{N_a h} \exp\left(\frac{\Delta S_a}{R}\right) \exp\left(\frac{-\Delta H_a}{RT}\right) \tag{6}$$

$$\mathrm{Ln}\left(\frac{G}{T}\right) = \mathrm{Ln}\left(\frac{R}{N_a h}\right) + \left(\frac{\Delta S_a}{R}\right) + \left(\frac{-\Delta H_a}{RT}\right) \tag{7}$$

$$\Delta G_a = \Delta H_a - T\Delta S_a \tag{8}$$

where G is the rheological behavior (Pa), G_0 is the constant (Pa), E_a is the activation energy (Kj mol^{-1}), R is the perfect gas constant (mol^{-1} K^{-1}) and T is the temperature (K).

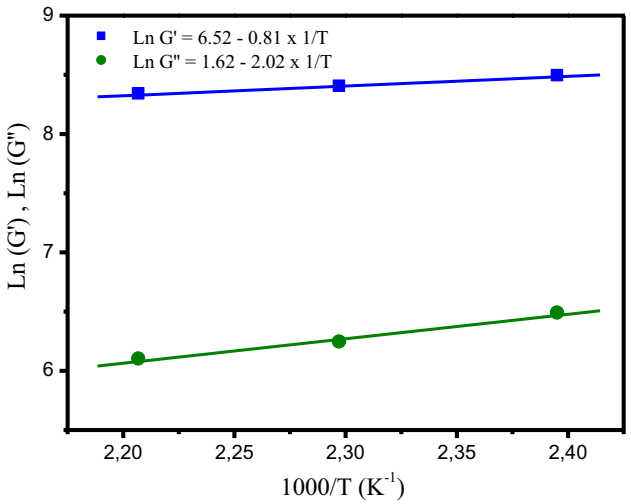

Fig. 8 Ln (G′) and Ln (G″) according to 1000/T

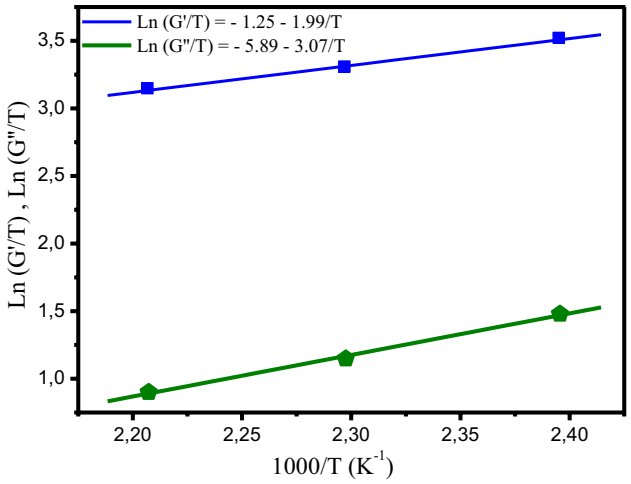

Fig. 9 Ln (G′/T) and Ln (G″/T) according to 1000/T

Figure 8 presents the Ln (G′) and Ln (G″) according to 1000/T, respectively. Furthermore, the Ln (G′/T) and Ln (G″/T) according to 1000/T are shown in Fig. 9.

From Figs. 8 and 9 and Eqs. 7 and 8, we determined the value of the activation energies, the activation enthalpy variation ΔH_a, the activation entropy variation ΔS_a and the activation of free energy variation ΔG_a of the pentafunctional epoxy resin (PGEPBAP) concerning the storage modulus G′ and loss modulus G″, respectively. These parameters are given in Table 2. The negative values of the activation enthalpy variation ΔH_a of the storage modulus and loss modulus mean that the reactions are exothermic. This is due to the heat provided by the apparatus which accelerates the process of the degradation of the pentafunctional phosphoric epoxy resin [9].

3.7.3 Storage modulus G′ and loss modulus G″ according to frequency

Figure 10 shows the storage modulus G′ and the loss modulus G″ of the elaborated composite (PGEPBAP/MDA/PN) according to the frequency at different formulations (0%, 5%, 10% and 15%) respectively. These rheological behaviors (G′ and G″) increase with the increase of the frequency and also with the rate of the charge of the natural phosphate incorporated in the composite (PGEPBAP/MDA/PN) [23, 24].

Table 2 Thermodynamic parameters

Rheological behaviors	E_a (Kj/mol)	ΔH_a (Kj/mol)	ΔS_a (Kj/mol)	ΔG_a (Kj/mol)
G′	− 6.734	− 16.544	− 208.26	− 66.453
G′	− 16.794	− 25.523	− 246.842	− 68.674

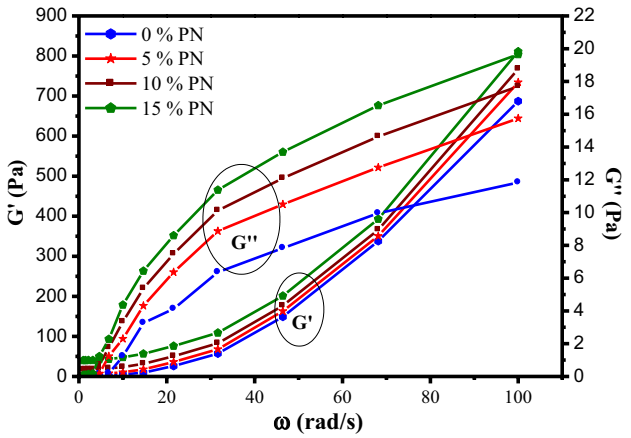

Fig. 10 Storage modulus and loss modulus of composite (PGEPBAP/MDA/PN) according to frequency at different formulations

These latter are studied using a RHM01-RD HAAKE rheometer type. Then, the storage modulus and loss modulus are in agreement with the results obtained by Bekhta et al. [25] for the dispersion of the charge, and by Fan and Advani [26] which showed that the rheological properties depend on the method of this dispersion due to the formulation of the composite (PGEPBAP/MDA/PN) which is well cured.

3.7.4 Morphology of composite (PGEPBAP/MDA/PN)

The morphology of different elaborated composite (PGEPBAP/MDA/PN) without and with natural phosphate incorporated in the epoxy matrix was determined by using the polarizing optical microscope (Fig. 11) [27, 28]. The morphology of the prepared composite varied greatly with the different percentages of the natural phosphate incorporated into pentafunctional epoxy resin PGEPBAP. Finally, the natural phosphate is well dispersed in the various composite (PGEPBAP/MDA/PN) [29, 30].

4 Conclusion

The pentafunctional epoxy resin PGEPBAP has been identified by Fourier transform infrared spectroscopy (FTIR) and nuclear magnetic resonance (^{1}H NMR, ^{13}C NMR and ^{31}P NMR). Moreover, the analysis of the viscosity of (PGEPBAP/Methanol) system shows that the viscosity increases with the percentage mass and decreases with the temperature. Furthermore, we proceeded the analysis of the rheological behaviors of PGEPBAP epoxy resins and their (PGEPBAP/MDA/PN) composite. Then, the results obtained concerning the temperature-dependence of storage and loss modulus indicate the necessity to store the epoxy matrix at low temperature. Additionally, the morphology of different prepared composites (PGEPBAP/MDA/PN) shows the very good dispersion of the natural phosphate as a filler.

Acknowledgements I would like to thank Professor Abderrahim El Bachiri, Doctor Mehdi El Bouchti and Salma Kantouch who collaborated to the success of this paper.

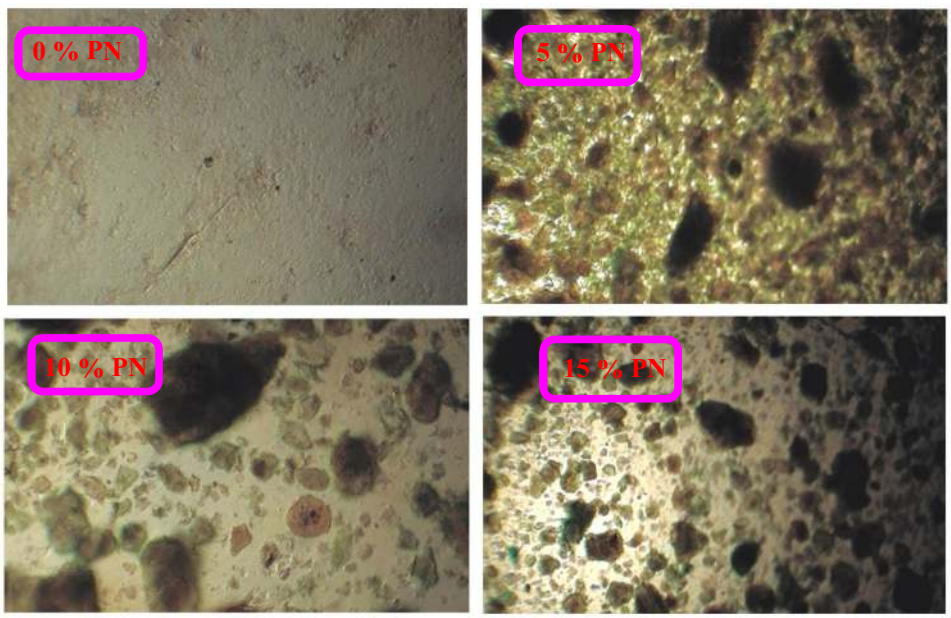

Fig. 11 Morphology of composite (PGEPBAP/MDA/PN) at different formulation

Compliance with ethical standards

Conflict of interest The authors declare that they have no competing interests.

References

1. Aghadavoudi F, Golestanian H, Zarasvand KA (2018) Elastic behaviour of hybrid cross-linked epoxy-based nanocomposite reinforced with GNP and CNT: experimental and multi-scale modelling. Polym Bull. https://doi.org/10.1007/s00289-018-2602-9
2. Hsissou R, About S, Berisha A, Berradi B, Assouag M, Hajjaji N, Elharfi A (2019) Experimental, DFT and molecular dynamics simulation on the inhibition performance of the DGDCBA epoxy polymer against the corrosion of the E24 carbon steel in 1.0 M HCl solution. J Mol Struct 1182:340–351
3. Ammar M, Chouaib A (2015) Mechanical and physicochemical characterization of an epoxy-based composite reinforced with fibrous biopolymer byproduct. Fibers Polym 16:2458–2466
4. Hsissou R, Bekhta A, Elharfi A (2017) Viscosimetric and rheological studies of a new trifunctional epoxy pre-polymer with noyan ethylene: triglycidyl Ether of Ethylene of Bisphenol A (TGEEBA). J Mater Environ Sci 8:603–610
5. Banafsheh S, Mostafa Y, Behzad R (2018) Rheological behavior of polypropylene/carbon quantum dot nanocomposites: the effects of particles size, particles/matrix interface adhesion, and particles loading. Polym Bull 76:4335–4354. https://doi.org/10.1007/s00289-018-2611-8
6. Hsissou R, Elharfi A (2018) Rheological behavior of three polymers and their hybrid composites (TGEEBA/MDA/PN), (HGEMDA/MDA/PN) and (NGHPBAE/MDA/PN). J King Saud Univ Sci. https://doi.org/10.1016/j.jksus.2018.04.030
7. Zoukrami F, Haddaoui N, Sclavons M, Devaux J, Vanzeveren C (2018) Rheological properties and thermal stability of compatibilized polypropylene/untreated silica composites prepared by water injection extrusion process. Polym Bull 75:5551–5566. https://doi.org/10.1007/s00289-018-2344-8
8. Revathi RK, Hariharan A, Prabunathan P, Srinivasan K, Alagar M (2018) Multifunctional behavior of POSS-reinforced imidazole core polyimide nanocomposites. Polym Bull. https://doi.org/10.1007/s00289-018-2636-z
9. Hsissou R, Berradi M, El Bouchti M, El Bachiri A, Elharfi A (2018) Synthesis characterization rheological and morphological study of a new epoxy resin pentaglycidyl ether pentaphenoxy of phosphorus and their composite (PGEPPP/MDA/PN). Polym Bull. https://doi.org/10.1007/s00289-018-2639-9
10. Fetouaki S, Elharfi A, Belkebir L (2002) Synthesis of a new epoxy resin based on 2,2′-dihydroxydiphenol. J Euro Polym 38:787–793
11. Hsissou R, Bekhta A, Elharfi A, Benzidia B, Hajjaji N (2018) Theoretical and electrochemical studies of the coating behavior of a new epoxy polymer: hexaglycidyl ethylene of methylene dianiline (HGEMDA) on E24 steel in 3.5% NaCl. Port Electrochim Acta 36:101–117
12. Hsissou R, Bekhta A, Elharfi A (2018) Synthesis and characterization of a new epoxy resin homologous of DGEBA: diglycidyl bis disulfide carbon ether of bisphenol A. J Chem Technol Metall 53:414–421
13. Hsissou R, El Bouchti M, Elharfi A (2017) Elaboration and viscosimetric, viscoelastic and rheological studies of a new hexafunctional polyepoxide polymer: hexaglycidyl ethylene of methylene dianiline. J Mater Environ Sci 8:4349–4361
14. Fernandes TMD, de Almeida JFM, Escócio VA, Silva ALN, de Sousa AMF, Visconte LLY, Furtado CRG, Pacheco EBAV, Laite MCA (2018) Evaluation of rheological behavior, anaerobic and thermal degradation, and lifetime prediction of polylactide/poly(butylene adipate-co-terephthalate)/powdered nitrile rubber blends. Polym Bull 76:2899–2913. https://doi.org/10.1007/s00289-018-2529-1
15. Solomon MJ, Amulsalam AS, Seefeldt KF, Somwangthanaroj A, Varadan P (2001) Rheology of polypropylene/clay hybrid materials. J Macromol 34:1864–1872
16. Vermant J, Ceccia S, Dolgovskij MK, Maffettone LP, Macosko CW (2007) Quantifying dispersion of layered nanocomposites via melt rheology. J Rheol 51:429–450
17. Ali HAM, Soliman HS, Saadeldin M, Sawaby K (2014) Frequency dependence of dielectric properties and conductivity of bulk copper sulfide. Mater Sci Semicond Process 18:141–145
18. Sousa FM, Costa ARM, Reul LT, Cavalcanti FB, Carvalho LH, Almeida TG, Canedo EL (2018) Rheological and thermal characterization of PCL/PBAT blends. Polym Bull 76:1573–1593. https://doi.org/10.1007/s00289-018-2428-5
19. Hsissou R, Elharfi A (2018) Elaboration and rheological study of a new trifunctional polyepoxide macromolecular binder. J Chem Technol Metall 53:170–176
20. Arfin T, Mohammad F (2013) DC electrical conductivity of nanocomposite polystyrene-titanium-arsenate membrane. J Ind Eng Chem 19:2046–2051
21. Nazari B, Kumar V, Bousfeild DW, Toivakka M (2016) Rheology of cellulose nanofibers suspensions: boundary driven flow. J Rheol 60:1151–1160
22. Zhijun N, Wei Y, Chixing Z (2016) Nonlinear rheological behavior of multiblock copolymers under large amplitude oscillatory shear. J Rheol 60:1161–1180
23. Momeni A, Filiaggi MJ (2016) Rheology of polyphosphate coacervates. J Rheol 60:25–34
24. Abdennadher A, Vincent M, Budtova T (2016) Rheological properties of molten flax- and Tencel polypropylene composites: influence of fiber morphology and concentration. J Rheol 60:191–202
25. Bekhta A, Hsissou R, El Bouchiti M, Elharfi A (2016) Synthesis, structural, viscosimetric and rheological study, of new trifunctional phosphorus epoxy prepolymer, triglycidyl ether trimercapto ethanol of phosphore (TGETMEP). Mediter J Chem 6:665–673
26. Fan Z, Advani SG (2007) Rheology of multiwall carbon nanotube suspensions. J Rheol 51:585–604
27. Ahmadi M, Rad-Moghadam K, Hatami M (2018) Investigation of morphological aspects and thermal properties of ZnO/poly(amide–imide) nanocomposites based on levodopa-mediated diacid monomer. Polym Bull 76:53–72. https://doi.org/10.1007/s00289-018-2366-2
28. Mohsen RM, Morsi SM, Selim MM, Ghoneim AM, El-Sherif HM (2018) Electrical, thermal, morphological, and antibacterial studies of synthesized polyaniline/zinc oxide nanocomposites. Polym Bull 76:1–21. https://doi.org/10.1007/s00289-018-2348-4
29. Prasad Rao J, Geckeler KE (2011) Polymer nanoparticles: preparation techniques and size-control parameters. Prog Polym Sci 36:887–913
30. Kodal M, Sirin H, Ozkoc G (2018) Long- and short-term stability of plasticized poly (lactic acid): effects of plasticizers type on thermal, mechanical and morphological properties. Polym Bull 76:423–445. https://doi.org/10.1007/s00289-018-2388-9